DOI: 10.2169/internalmedicine.47.0370

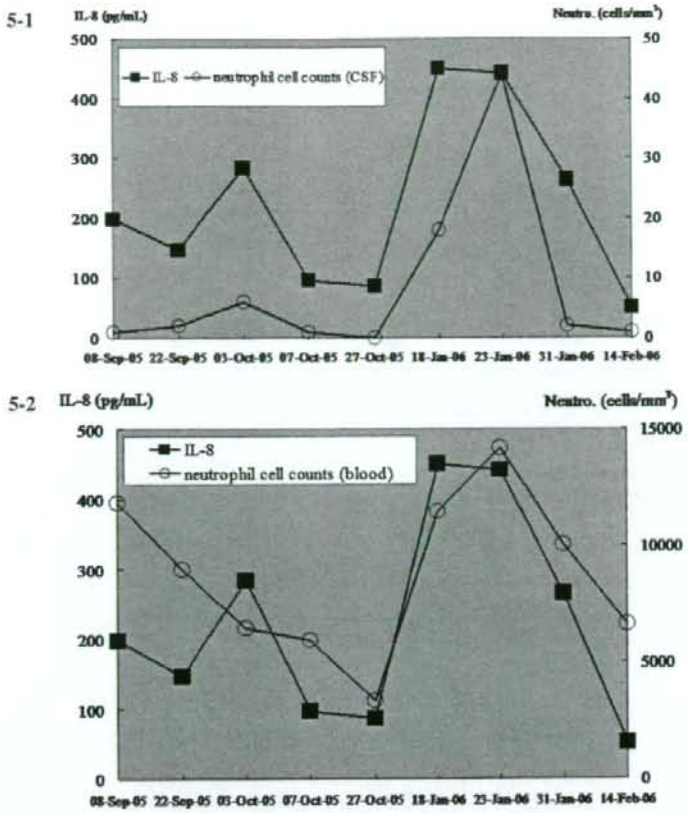

Figure 5. Correlation between level of IL-8 (pg/mL) in CSF and neutrophilic cell counts [(Neutro.), cells/mm³] in CSF (5-1) and peripheral blood (5-2).

was negative. 4. Antibiotics and antiviral therapy were not effective, but systemic glucocorticoids were so effective that the neurologic symptoms and laboratory findings markedly improved. 5. She did not display cutaneous vasculitis and thrombosis, which are seen in Behçet's disease. 6. Abnormal signal intensities on MRI were demonstrated in various CNS regions without site predilection.

The cytokines and chemokines in CSF that correlated well with the clinical state and total CSF cell counts were IL-6, IFN-γ, IL-8 and IP-10. CD4+ helper T (Th) cells can be divided into the Th1 and Th2 subtypes according to their cytokine secretion patterns (10-12). IFN-γ and IP-10, the levels of which increased in our patient, are Th1-type cytokines. Coincidentally, Th1-type cytokines have previously been implicated as mediators of the pathogenesis of Sweet's disease (13, 14). Our data suggest an important role of Th1 cells in the pathogenesis of NSD which is Sweet disease with CNS involvement. The levels of IL-4 and IL-10, which are Th2-type cytokines, were also statistically correlated with total CSF cell counts. However, the elevations of these cytokines were almost within normal ranges of control subjects. It is known that these cytokines in turn cause a decrease in the release of the Th1-type cytokines, thereby regulating the inflammatory response. We thought that the elevations of these cytokines were induced by the elevations of the Th1-type cytokines. IFN-γ causes overexpression of adhesion molecules, responsible for neutrophilic adherence and diapedesis (13). There are multiple reports that suggest that neutrophil chemotactic dysfunction may be the basis of Sweet disease (15-17). In this study, the level of IL-8, a specific neutrophil chemoattractant, correlated with the neutrophil cell count in CSF indicating that NSD may also result from neutrophil chemotactic dysfunction. The level of GM-CSF, a neutrophil chemoattractant similar to IL-8, was below the detection limits. We were therefore unable to show any correlation for this chemokine. The increases in the levels of cytokines and chemokines in the CSF of the patient at the second hospitalization were generally higher than those at the first hospitalization. This finding may be attributed to the delay of the systemic glucocorticoid therapy at the second hospitalization.

Recently, the differences between NSD and NBD have been discussed (2, 18, 19). The present patient did not fulfill the criteria of BD (20) and the HLA type (Cw1 and B54) and histology of a skin biopsy from our patient corresponded to NSD, but not to NBD (2). There are several reports of BD that demonstrate an elevation in the levels of Th1-type cytokines in the serum of patients in the active

phase (21, 22) and in turn suggest that IL-8 could be a serological marker of disease activity (23, 24). In addition, elevated levels of IFN-γ and IL-6 in CSF are detectable in patients in the active phase of NBD (25, 26). Our cytokine data suggested that there are common aspect of pathogenesis between NSD and NBD.

Therapy with systemic glucocorticoids is usually effective in improving the neurologic symptoms in patients with NSD; however, like our patient, some patients occasionally experience recurrent episodes of neurological manifestations after glucocorticoid therapy is discontinued (1). Preventive therapies have not been established, but our study demonstrates that the levels of the Th1 cytokines, IL-6 and IL-8 in CSF are important markers of disease activity in patients with NSD. It is known that the treatment with IFN-β reduces the amount of Th1 proinflammatory cytokines and shifts the immune response toward a Th2 profile (27). Therefore, this treatment might have the potential to prevent the reccurence of NSD. We believe that these results provide useful information for clarifying the pathogenesis of NSD, which may contribute to the development of future therapeutic strategies.

This research was partially supported by a Grant-in-Aid for Young Scientists (B), 1690486 from the Japanese Ministry of Education, Culture, Sports, Science and Technology, a Grant-in-Aid for Scientific Research INo. 17591133 and a Health and Labor Sciences Research Grant for Research on Psychiatry and Neurological Diseases and Mental Health (H18-026).

References

1. Hisanaga K, Hosokawa M, Sato N, Mochizuki H, Itoyama Y, Iwasaki Y. "Neuro-Sweet disease": Benign recurrent encephalitis with neutrophilic dermatosis. Arch Neurol **56**: 1010-1013, 1999.
2. Hisanaga K, Iwasaki Y, Itoyama Y, Neuro-Sweet Disease; Study Group. Neuro-Sweet disease: Clinical manifestations and criteria for diagnosis. Neurology **64**: 1756-1761, 2005.
3. Mizoguchi M, Matsuki K, Mochizuki M, et al. Human leukocyte antigen in Sweet's syndrome and its relationship to Behçet's disease. Arch Dermatol **124**: 1069-1073, 1998.
4. Noda K, Okuma Y, Fukae J, et al. Sweet's syndrome associated with encephalitis. J Neurol Sci **188**: 95-97, 2001.
5. Druschky A, von den Dreisch P, Anders M, Claus D, Neundorfer B. Sweet's sndrome (acute febrile neutrophilic dermatosis) affecting the central nervous system. J Neurol **243**: 556-557, 1996.
6. Chen R, Lowe L, Wilson JD, et al. Simultaneous quantification of six human cytokines in a single sample using microparticle-based flow cytometric technology. Clin Chem **45**: 1693-1694, 1999.
7. Cook EB, Stahl JL, Lowe L, et al. Simultaneous measurement of six cytokines in a single sample of human tears using microparticle-based flow cytometry: allergics vs. non-allergics. J Immunol Methods **254**: 109-118, 2001.
8. Metelitsa LS, Naidenko OV, Kant A, et al. Human NKT cells mediate antitumor cytotoxicity directly by recognizing target cell CD1d with bound ligand or indirectly by producing IL-2 to activate NK cells. J Immunol **167**: 3114-3122, 2001.
9. Nakajima H, Fukuda K, Doi Y, et al. Expression of TH1/TH2-related chemokine receptors on peripheral T cells and correlation with clinical disease activity in patients with multiple sclerosis. Eur Neurol **52**: 162-168, 2004.
10. Romagnani S. The Th1/Th2 paradigm. Immunol Today **18**: 263-266, 1997.
11. Mosmann TR, Coffman RL. Th1 and Th2 cells: different patterns of lymphokine secretion lead to different functional properties. Annu Rev Immunol **7**: 145-173, 1989.
12. Abbas AK, Murphy KM, Sher A. Functional diversity of helper T lymphocytes. Nature **383**: 787-793, 1996.
13. Giasuddin AS, El-Orfi AH, Ziu MM, El-Barnawi NY. Sweet's syndrome: Is the pathogenesis mediated by helper T cell type 1 cytokines? J Am Acad Dermatol **39**: 940-943, 1998.
14. Nifosi G. Sweet syndrome: personal experience and review of the literature. Minerva Med **92**: 49-55, 2001.
15. Park JW, Mehrotra B, Barnett BO, Baron AD, Venook AP. The Sweet syndrome during therapy with granulocyte colony-stimulating factor. Ann Intern Med **116**: 996-998, 1992.
16. Kumar G, Bernstein JM, Waibel JS, Baumann MA. Sweet's syndrome associated with sargramostim (granulocyte-macrophage colony stimulating factor) treatment. Am J Hematol **76**: 283-285, 2004.
17. Watarai K, Tojo A, Nagamura-Inoue T, et al. Hyperfunction of neutrophils in a patient with BCR/ABL negative chronic myeloid leukemia: a case report with in vitro studies. Cancer **89**: 551-560, 2000.
18. Iwatsuki K, Deguchi K, Narai H, et al. A case of neuro-Behçet's disease with HLA B54 and predominant cerebral white matter lesions. Rinsho Shinkeigaku **40**: 921-925, 2000 (in Japanese).
19. Uysal H, Vahaboglu H, Inan L, Vahaboglu G. Acute febrile neutrophilic dermatosis (Sweet's syndrome) in neuro-Behçet's disease. Clin Neurol Neurosurg **95**: 319-322, 1993.
20. International Study, Group for Behçet's Disease. Criteria for diagnosis of Behçet disease. Lancet **335**: 1078-1080, 1990.
21. Frassanito MA, Dammacco R, Cafforio P, Dammacco F. Th1 polarization of the immune response in Behçet's disease. A putative pathogenetic role of interleukin-12. Arthritis Rheum **42**: 1967-1974, 1999.
22. Raziuddin S, Al-Dalaan A, Bahabri S, Siraj AK, al-Sedairy S. Divergent cytokine production profile in Behçet's disease. Altered Th1/Th2 cell cytokine pattern. J Rheumatol **25**: 329-333, 1998.
23. al-Dalaan A, al-Sedairy S, al-Balaa S, et al. Enhanced interleukin 8 secretion in circulation of patients with Behçet's disease. J Rheumatol **22**: 904-907, 1995.
24. Gur-Toy G, Lenk N, Yalcin B, Aksaray S, Alli N. Serum interleukin-8 as a serologic marker of activity in Behçet's disease. Int J Dermatol **44**: 657-660, 2005.
25. Hirohata S, Isshi K, Oguchi H, et al. Cerebrospinal fluid interleukin-6 in progressive neuro-Behçet's syndrome. Clin Immunol Immunopathol **82**: 12-17, 1997.
26. Hirayama M, Kiyosawa K, Nakazaki S, Fujiki N, Iida M. Measurement of gamma-interferon in sera and CSF in patients with multiple sclerosis and inflammatory neurological diseases. Rinsho Shinkeigaku **30**: 557-559, 1990 (in Japanese).
27. Markowiitz CE. Interferon-beta: Mechanism of action and dosing issues. Neurology **68**: 8-11, 2007.

Lupus (2008) 17, 16–20
http://lup.sagepub.com

PAPER

Proteomic analysis of autoantibodies in neuropsychiatric systemic lupus erythematosus patient with white matter hyperintensities on brain MRI

A Kimura[1]*, T Sakurai[1], Y Tanaka[1], I Hozumi[1], K Takahashi[2], M Takemura[2], K Saito[2], M Seishima[2] and T Inuzuka[1]

[1]Department of Neurology and Geriatrics, Gifu University Graduate School of Medicine, Gifu City, Gifu, Japan; and
[2]Department of Informative Clinical Medicine, Gifu University Graduate School of Medicine, Gifu City, Gifu, Japan

The pathogenesis of neuropsychiatric systemic lupus erythematosus (NPSLE) may be related to autoantibody-mediated neural dysfunction, vasculopathy and coagulopathy. We encountered an NPSLE patient whose brain showed characteristic diffuse symmetrical hyperintensity lesions in the cerebral white matter, cerebellum and middle cerebellar peduncles on T2-weighted magnetic resonance (MR) images. In this study, we investigated all the antigens that reacted strongly with autoantibodies in this patient's serum by two-dimensional electrophoresis (2DE), followed by western blotting (WB) and liquid chromatography-tandem mass spectrometry (LC-MS/MS) using rat brain proteins as the antigen source. As a result, we identified four antigens as beta-actin, alpha-internexin, 60 kDa heat-shock protein (Hsp60) and glial fibrillary acidic protein (GFAP). There are several reports on the detection of anti-endothelial cell antibodies (AECAs) in an SLE patients. Recently, one of the antigens reacting with AECAs in SLE patient's sera has been identified as human Hsp60. We speculated that the abnormal findings on brain MR images of our patient may be due to impairment of microcirculation associated with vascular endothelial cell injury mediated by the antibody against Hsp60. This proteomic analysis is a useful tool for identifying autoantigens in autoimmune diseases involving autoantibodies. *Lupus* (2008) **17**, 16–20.

Key words: endothelial cell; 60 kDa heat shock protein (Hsp60); neuropsychiatric systemic lupus erythematosus (NPSLE); proteome; white matter hyperintensity (WMH)

Introduction

Patients with neuropsychiatric systemic lupus erythematosus (NPSLE) frequently show various abnormal findings including white matter hyperintensities (WMHs) on T2-weighted brain magnetic resonance (MR) images.[1–3] White matter hyperintensities appear to represent asymptomatic cerebral small vessel disease (SVD).[4] There is accumulating evidence that WMHs are associated with several impairments such as cognitive deficits.[5–7] The pathogenesis of cerebral SVD is poorly understood, but endothelial activation and dysfunction may play a causal role.[4]

Here, we report the case of an NPSLE patient, whose brain MRI showed characteristic WMHs on T2-weighted and fluid-attenuated inversion recovery (FLAIR) images. We examined the reactivity of his serum antibodies against rat brain antigens using the two-dimensional immunoblotting method and identified the antigens that reacted with these autoantibodies by the proteomic method.

Materials and methods

Patient and serum samples

Serum samples were collected from an untreated 69-year old male patient with NPSLE. His clinical features are summarized as follows:

1. He showed slowly progressive polyneuropathy predominantly in the lower limbs and subsequent

*Correspondence: Dr Akio Kimura, Department of Neurology and Geriatrics, Gifu University Graduate School of Medicine, Gifu, 1-1 Yanagido, Gifu City, Gifu 501-1194, Japan. E-mail: kimura1@gifu-u.ac.jp
Received 28 July 2007; accepted 18 September 2007

10.1177/0961203307085112

encephalopathy one year after the onset of polyneuropathy.

2. Proteinuria was detected by urinalysis and membranous nephropathy was demonstrated by renal biopsy.
3. Our patient presented delusion and hallucination without insight. Disorientation of time and place were noted. His recent memory was impaired, as he was unable to recall any of three objects after 5 min. He showed impairment of complex attention [disability of digit span (backward)]. Our patient's neurological symptoms were cognitive dysfunction, psychosis and polyneuropathy, as determined on the basis of American College of Rheumatology (ACR) Nomenclature on the NPSLE.[8]
4. Laboratory tests revealed the presence of several autoantibodies [anti-nuclear antibody, anti-DNA antibody, anti-Sm antibody, anti-RNP antibody and lupus anti-coagulant (dRVVT 1.31: normal <1.3)]; hyperglobulinemia [IgG (3448 mg/dL, normal 890–1850 mg/dL)]; decreases in the levels of complements [CH50 (16.9 CH50U/mL, normal 23–46 CH50U/mL) and C4 (2 mg/dL, normal 12–30 mg/dL)], white blood cell count (3620/μl, normal 3400–9200/μl) and lymphocyte cell count (1340/μl, normal 646–4177/μl); and coagulation-fibrinolysis abnormalities [increases in the levels of fibrinogen/fibrin degradation products (FDP) (11.3 μg/mL, normal ≤4.0 μg/mL), D-dimer (1.5 μg/mL, normal ≤1.0 μg/mL) and alpha2-plasmin inhibitor-plasmin complex (PIC) (1.4 μg/mL, normal ≤0.8 μg/mL) and decreases in the value of the thrombotest (48%, normal 70–150%), fibrinogen level (150 mg/dL, normal 150–350 mg/dL), anti-thrombin III activity (71%, normal 80–130%), protein C activity (58%, normal 64–146%), protein C antigen level (61%, normal 70–150%) and protein S activity (52%, normal 60–150%)].
5. Brain MRI showed characteristic diffuse symmetrical hyperintensity lesions in the cerebral white matter, cerebellum and middle cerebellar peduncles on T2-weighted and FLAIR images (Figure 1). Diffusion-weighted images (DWIs) showed high intensities in the bilateral middle cerebellar peduncles with decreased apparent diffusion coefficient (ADC) values. These findings on DWIs and the ADC map suggest that the lesions represent cytotoxic edema caused by ischemic changes.
6. The findings of a nerve conduction study revealed sensory motor axonal degeneration predominantly in the lower limb.

The above-mentioned findings fulfilled the ACR criteria on SLE.[9] He had no risk factors for atherosclerosis, such as hypertension, hyperlipidemia and diabetes mellitus.

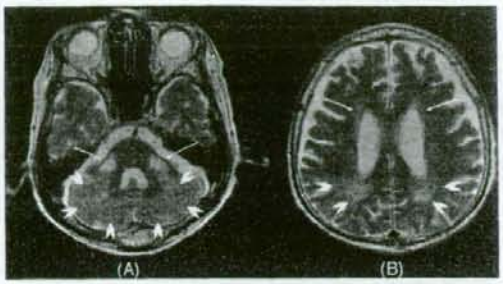

Figure 1 , T2-weighted brain MR images (SE, TR/TE: 4080/100 ms). Brain MRI showed symmetrical hyperintensity lesions in bilateral cerebellar hemispheres (arrowheads), middle cerebellar peduncles (arrows) (A), periventricular white matter (arrows) and (B), deep white matter (arrowheads).

Preparation of tissue proteins

Under ether anesthesia, adult Sprague-Dawley rats were sacrificed. The cerebrums were immediately removed and frozen in dry-ice powder. The frozen brain tissue was homogenized with a tissue homogenizer in lysis solution, consisting of 20 mM Tris, 7M urea, 2M thiourea, 4% CHAPS, 10 mM 1,4-dithioerythritol (DTT), 1 mM EDTA and 1 mM phenylmethylsulfonyl fluoride containing a cocktail of protease inhibitors (Calbiochem, San Diego, CA, USA). The homogenate was centrifuged at 150 000 × g for 45 min and the supernatant was used in all experiments. Protein concentration was determined by Bio-Rad Protein assay based on the Bradford method (Bio-Rad Laboratories, Hercules, CA, USA).

Two-dimensional electrophoresis

The samples were dissolved in destreak rehydration solution (GE Healthcare, Buckinghamshire, UK) and loaded by in-gel rehydration into 7-cm long immobilized pH gradient dry strips (GE Healthcare, Buckinghamshire, UK). Up to 250 μg of extracted proteins was applied to the dry strips for Western blotting (WB). Isoelectric focusing was conducted at 20°C for 24 000 Vh at a maximum of 5000 V using a horizontal electrophoresis system, Multiphor III (GE Healthcare, Buckinghamshire, UK). Before separation in the second dimension, the IPG strips were equilibrated for 15 min in a buffer containing 2% SDS, 6M Urea, 30% v/v glycerol, 0.001% BPB and 50 mM Tris-HCl (pH 8.8) under reducing conditions with 65 mM DTT, followed by incubation for 15 min in the same buffer

under alkylating conditions with 140 mM iodoacetamide. Equilibrated IPG strips were transferred to a 12.5% polyacrylamide gel and run at 15 mA/gel. After the electrophoresis, the SDS-PAGE gels were stained with Coomassie Brilliant Blue (GelCode Blue Stain Reagent, Pierce) or used for protein transfer onto polyvinylidine difluoride (PVDF) membranes.

Immunoblotting

Separated proteins were electrophoretically transferred to a PVDF membrane at 50 volts for 3 h using a buffer transfer tank with cold equipment. The PVDF membrane was incubated in blocking solution (5% skim milk in 1 × TBST; 1 × TBS containing 0.1% Tween 20) overnight in a cold room and then reacted with the patient's serum diluted (1:1000) in 1% skim milk in 1 × TBST for 1 h at room temperature. The PVDF membrane was washed five times with 1 × TBST and reacted with peroxidase-conjugated goat anti-human Ig (A + G + M) antibodies (P.A.R.I.S, France) diluted (1:1000) with 1% skim milk in 1 × TBST for 1 h at room temperature. After six washes, the membrane was incubated with the ECL reagent for 1 min and then exposed to an x-ray film for 15–300 s.

Gel digestion and mass spectrometry

The target spot was excised from the gel and subjected to trypsin digestion and peptide fragments were analysed using a nanoscale capillary LC system (LV-VP, Shimadzu) and an ion trap tandem mass spectrometer (LCQ Advantage Max, Thermo Electron). Proteins were identified from MS/MS spectra using protein identification software (X calibur TM, Thermo Finnigan and MASCOT Search, Matrix Science).

Determination of anti-60 kDa heat shock protein antibodies

We determined by enzyme-linked immunosorbent assay (ELISA) the titers of anti-Hsp60 antibodies in sera from our patient, patients with NPSLE (n = 5: age range, 22–58; mean age, 42.4) without abnormal WMHs and healthy controls without abnormal WMHs (n = 7; age range, 17–67; mean age, 43.1). We carried out ELISA to analyse the reactivities of autoantibodies against human Hsp60, which were measured using an ELISA kit (Stressgen, Ann Arbor, MI, USA). Sera diluted 1:1000 in a dilution buffer were added to a precoated ready-to-use recombinant human Hsp60 immunoassay plate and then incubated for 2 h at room temperature (RT). After four washes, peroxidase-conjugated anti-human IgG, A or M was added to each well and then incubated for 1 h at RT. After four washes, a stabilized tetrametylbenzidine substrate was added to each well and then incubated for 15 min at RT. The reaction was stopped by adding acid stop solution and the plate was read at 450 nm on a microplate reader. The OD of control wells without Hsp60 was subtracted from the OD of Hsp60-coated wells. Serial dilutions of serum samples of healthy blood donors having high antibody levels against the tested Hsp60 were used as standards.

Results

Screening and identification of target proteins that reacted with autoantibodies in patient's serum

We detected nine spots (pI 4.2–124 kDa, pI 5.15–kDa, pI 5.3–53 kDa, pI 5.4–53 kDa, pI 5.5–53 kDa, pI 5.25–57 kDa, pI 5.4–57 kDa, pI 5.15–63 kDa, pI 8.0–35 kDa) that strongly reacted with autoantibodies in patient's serum on 2DE-WB (Figure 2). Five among the nine spots that matched proteins on 2-DE gels were analysed by LC-MS/MS. These immunoreactive proteins were identified as beta-actin (pI 5.15–46 kDa), alpha-internexin (pI 5.15–63 kDa), Hsp60 (pI 5.25–57 kDa and pI 5.4–57 kDa) and glial fibrillary acidic protein (GFAP) (pI 5.3–53 kDa) (Table 1).

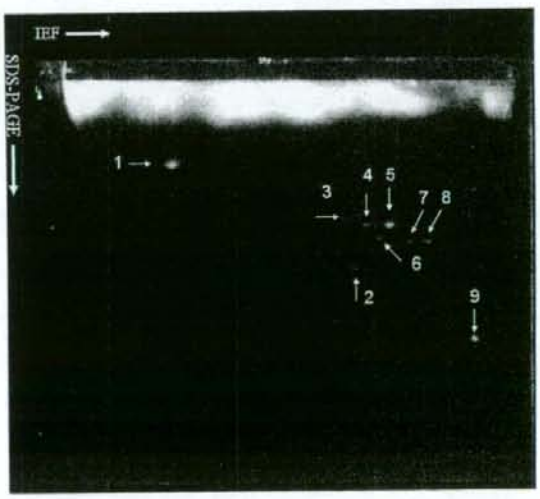

Figure 2 Two-dimensional electrophoresis (2DE) and western blotting (WB). Nine spots strongly reacted with autoantibodies in patient's serum on 2DE-WB. Five spots (No. 2–6) were analysed using mass spectrometry. No. 2: Beta actin; No. 3: Alpha-internexin; No. 4 and 5: 60 kD heat-shock protein (Hsp60); No. 6: Glial fibrillary acidic protein (GFAP); No. 1, 7, 8 and 9: no identification was made.

Table 1 Autoantigens identified using mass spectrometry

Spot Number[a]	*Protein name*	*Mascot score*	*Number of peptides*	*Coverage%*	*Observed M.W.(kDa) /pI*	*Calculated M.W.(kDa) /pI*
2	Beta-actin	421	16	41	46/5.15	42/5.29
3	Alpha-Inx[b]	203	5	12	63/5.15	56/5.20
4	Hsp 60[c]	112	3	6	57/5.25	61/5.91
5	Hsp 60	112	3	8	57/5.4	61/5.91
6	GFAP[d]	113	2	2	53/5.3	50/5.35

[a]Spot number corresponds to the number shown in Figure 2.
[b]Alpha-Inx, Alpha-internexin.
[c]Hsp 60, 60 kD heat-shock protein.
[d]GFAP, Glial fibrillary acidic protein.

Detection of anti-Hsp60 antibodies in our patient and controls

The titer of the anti-Hsp60 antibody in our patient was 133.6 ng/mL. The mean titer of this antibody in five NPSLE patients without WMHs on brain MR images was 19.72 (SD 10.65; range 9.0–32.2) ng/mL. The mean titer of this antibody in the seven healthy controls without WMHs on brain MR images was 15.36 (SD 11.85; range 5.7–39.5) ng/mL.

Discussion

In this study, we detected some autoantigenic proteins reacting with autoantibodies in a serum sample from a patient with NPSLE using the proteomic approach and we identified four autoantigens, namely, beta-actin, alpha-internexin, Hsp60 and GFAP. There are some previous studies demonstrating the association of autoantibodies in serum and cerebrospinal fluid (CSF) with central nervous system involvement in patients with NPSLE.[10–12] Anti-endothelial cell antibodies (AECAs) have been detected in SLE patients.[13,14] Recently, one of the antigens that reacted with AECAs in a SLE patient's sera has been identified as human Hsp60.[15] Human Hsp60 is a molecular chaperone that participates in the folding of mitochondrial proteins and facilitates proteolytic degradation of misfolded or denatured proteins.[16] However, it has also been reported that an enhanced expression of this protein on endothelial cells has been noted and antibodies against human Hsp60 induce endothelial cell toxicity.[15,17,18]

Our patient's brain MR images showed characteristic cerebral WMHs, which appear to represent cerebral SVD. The pathogenesis of cerebral SVD is poorly understood, but endothelial activation and dysfunction may play a causal role.[4] It has been reported that the anti-Hsp60 antibody is present in most patients with coronary artery disease that its titer correlates with disease severity[19] and that it may contribute to the initiation or amplification of vascular endothelial cell damage in atherosclerosis, which is considered a crucial event.[20] Our patient's laboratory findings showed a slightly high level of lupus anticoagulant and some coagulation-fibrinolysis abnormalities. It has been reported that the anti-Hsp60 antibody bind to endothelial cells and induce a thrombotic cascade following endothelial cell apoptosis in SLE patients with the anti-phospholipid antibody.[15] In this study, we determined by ELISA the titer of the anti-Hsp60 antibody in sera from our patient and controls without WMHs on brain MR images. The titer of this antibody in serum from our patient was markedly higher than the mean +2SD of NPSLE patients without WMH or that of healthy controls without WMHs. Thus, the abnormal WMH lesions on brain MR images in our patient may be at least partially due to the impairment of microcirculation associated with vascular endothelial cell dysfunction mediated by the antibody against Hsp60. Further studies using a large series of controls are required to clarify the relationship between the anti-Hsp60 antibody and WMHs on brain MR images.

On the other hand, the clinical significance of the anti-GFAP antibody in NPSLE remains controversial. There is a report showing that the anti-GFAP antibody is specific for NPSLE.[2] Another report suggested that GFAP might be a useful marker in the diagnosis and monitoring of NPSLE, because GFAP level increases in the CSF of NPSLE.[21] However, Valesini *et al.*[22] have reported that the presence of the anti-GFAP antibody in sera of SLE patients showed no significant correlation with neurologic or psychiatric morbidity. Further study will be necessary to clarify the association between the anti-GFAP antibody and NPSLE.

Previously, there were several reports, which described that the autoantibodies against beta-actin and alpha-internexin were detected from non-neurological diseases or healthy controls.[23,24] Therefore, we thought that these autoantibodies were not specifically related to NPSLE and are parts of the natural autoantibody repertoire.

In this study, we detected several autoantibodies from our NPSLE patient and identified the autoantigens that they reacted. Several autoantibodies are generated in systemic autoimmune diseases, and an understanding of the interaction among these

autoantibodies will help clarify their pathogenesis. The proteomic analysis used in our study is a very useful tool for identifying several autoantigens reacting with autoantibodies at one time.

Acknowledgements

This research was partially supported by a Japanese Health and Labour Sciences Research Grant for Research on Psychiatry and Neurological Diseases and Mental Health (H18-026, H17-017) and a Grant-in-Aid for Young Scientists (B), 1690486 from the Japanese Ministry of Education, Culture, Sports, Science and Technology and a Grant-in-Aid for Scientific Research No. 17591133.

References

1 Bell CL, Partington C, Robbins M, Graziano F, Turski P, Kornguth S. Magnetic resonance imaging of central nervous system lesions in patients with lupus erythematosus. Correlation with clinical remission and antineurofilament and anticardiolipin antibody titers. *Arthritis Rheum* 1991; **34**: 432–441.

2 Sanna G, Piga M, Terryberry JW *et al.* Central nervous system involvement in systemic lupus erythematosus: cerebral imaging and serological profile in patients with and without overt neuropsychiatric manifestations. *Lupus* 2000; **9**: 573–583.

3 Hachulla E, Michon-Pasturel U, Leys D *et al.* Cerebral magnetic resonance imaging in patients with or without antiphospholipid antibodies. *Lupus* 1998; **7**: 124–131.

4 Markus HS, Hunt B, Palmer K, Enzinger C, Schmidt H, Schmidt R. Markers of endothelial and hemostatic activation and progression of cerebral white matter hyperintensities. Longitudinal results of the Austrian stroke prevention study. *Stroke* 2005; **36**: 1410–1414.

5 Gunning-Dixon FM, Raz N. The cognitive correlates of white matter abnormalities in normal aging: a quantitative review. *Neuropsychology* 2000; **14**: 224–232.

6 Sachdev PS, Wen W, Christensen H, Jorm AF. White matter hyperintensities are related to physical disability and poor motor function. *J Neurol Neurosurg Psychiatry* 2005; **76**: 362–367.

7 Mosley TH, Knopman DS, Catelier DJ *et al.* Cerebral MRI findings and cognitive functioning. The atherosclerosis risk in communities study. *Neurology* 2005; **64**: 2056–2062.

8 ACR Ad Hoc Committee On Neuropsychiatric Lupus Nomenclature. The American College of Rheumatology nomenclature and case definitions for neuropsychiatric lupus syndromes. *Arthritis Rheum* 1999; **42**: 599–608.

9 Hochbreg MC. Updating the American College of Rheumatology revised criteria for the classification of systemic lupus erythematosus. *Arthritis Rheum* 1997; **40**: 1725.

10 Bluestein HG, Zvaifler NJ. Brain-reactive lymphocytotoxic antibodies in the serum of patients with systemic lupus erythematosus. *J Clin Invest* 1976; **57**: 509–516.

11 Bonfa E, Golombek SJ, Kaufman LD *et al.* Association between lupus psychosis and anti-ribosomal P protein antibodies. *N Engl J Med* 1987; **317**: 265–271.

12 Isshi K, Hirohata S. Differential roles of the anti-ribosomal P antibody and antineuronal antibody in the pathogenesis of central nervous system involvement in systemic lupus erythematosus. *Arthritis Rheum* 1982; **25**: 1271–1277.

13 Song J, Park YB, Lee WK, Lee KH, Lee SK. Clinical associations of anti-endothelial cell antibodies in patients with systemic lupus erythematosus. *Rheumatol Int* 2000; **20**: 1–7.

14 Meroni PL, Tincani A, Sepp N *et al.* Endothelium and the brain in CNS lupus. *Lupus* 2003; **12**: 919–928.

15 Dieudé M, Senécal JL, Raymond Y. Induction of endothelial cell apoptosis by heat-shock protein 60-reactive antibodies from anti-endothelial cell autoantibody-positive systemic lupus erythematosus patients. *Arthritis Rheum* 2004; **50**: 3221–3231.

16 Martin J, Horwich AL, Hartl FU. Prevention of protein denaturation under heat stress by the chaperonin Hsp60. *Science* 1992; **258**: 995–998.

17 Jamin C, Dugué C, Alard JE *et al.* Induction of endothelial cell apoptosis by the binding of anti-endothelial cell antibodies to Hsp60 in vasculitis-associated systemic autoimmune diseases. *Arthritis Rheum* 2005; **52**: 4028–4038.

18 Schett G, Xu Q, Amberger A *et al.* Autoantibodies against HSP60 mediate endothelial cytotoxicity. *J Clin Invest* 1995; **96**: 2569–2577.

19 Zhu J, Katz RJ, Quyyumi AA *et al.* Antibodies to HSP60 are associated with the presence and severity of coronary artery disease: evidence for an autoimmune component of atherogenesis. *Circulation* 2001; **103**: 1071–1075.

20 Bason C, Corrocher R, Lunardi C *et al.* Interaction of antibodies against cytomegalovirus with heat-shock protein 60 in pathogenesis of atherosclerosis. *Lancet* 2003; **362**: 1971–1977.

21 Trysberg E, Nylen K, Rosengren LE, Tarkowski A. Neuronal and astrocytic damage in systemic lupus erythematosus patients with central nervous system involvement. *Arthritis Rheum* 2003; **48**: 2881–2887.

22 Valesini G, Alessandri C, Celestino D, Conti F. Anti-endothelial antibodies and neuropshychiatric systemic lupus erythematosus. *Ann NY Acad Sci* 2006; **1069**: 118–128.

23 Boulassel MR, Tomasi JP, Deggouj N, Gersdorff M. Identification of beta-actin as a candidate autoantigen in autoimmune inner ear disease. *Clin Otolaryngol* 2000; **25**: 535–541.

24 Rajasalu T, Teesalu K, Janmey PA, Uibo R. Demonstration of natural autoantibodies against the neurofilament protein α-internexin in sera of patients with endocrine autoimmunity and healthy individuals. *Immunol Lett* 2004; **94**: 153–160.

Clinical Neurology and Neurosurgery 111 (2009) 296–299

Contents lists available at ScienceDirect

Clinical Neurology and Neurosurgery

journal homepage: www.elsevier.com/locate/clineuro

Case report

Monofocal large inflammatory demyelinating lesion, mimicking brain glioma

Noriyuki Kimura*, Toshihide Kumamoto, Takuya Hanaoka, Yusuke Hasama, Kenichiro Nakamura, Toshio Okazaki

Department of Neurology and Neuromuscular Disorders, Oita University, Faculty of Medicine, Idaigaoka 1-1, Hasama, Yufu, Oita 879-5593, Japan

ARTICLE INFO

Article history:
Received 5 May 2008
Received in revised form 5 October 2008
Accepted 7 October 2008

Keywords:
Monofocal demyelinating lesion
Glioma
Brain MRI
Steroid therapy
Brain biopsy

ABSTRACT

Here we report two cases of pathologically confirmed tumor-like demyelinating lesions. In comparison with common primary demyelinating diseases, our cases demonstrated atypical radiologic features, such as a large monofocal lesion with mild brain edema, and open ring-like or focal enhancement on magnetic resonance images, suggesting brain tumors. The clinical manifestations included focal neurologic signs due to the lesions, monophasic episodes without relapse over a long follow-up period, and efficacy of oral corticosteroid therapy. Histological analysis of brain biopsy specimens showed the inflammatory demyelination and preserved axons without tumor cells. The present cases suggest the importance of considering inflammatory demyelinating disease in the different diagnosis of monofocal tumor-like lesion.

1. Introduction

A tumor-like demyelinating lesion is a rare and unique radiologic finding. They appear as a large monofocal or multifocal contrast-enhancing lesions, and are often indistinguishable from brain tumors on computed tomography or magnetic resonance imaging (MRI) [1,2]. The clinical findings of such lesions are characterized by a rapidly progressive clinical course and neurologic symptoms, such as headaches, seizures, and unconsciousness [3,5–7]. These findings often lead to an incorrect or delayed diagnosis and treatment. Thus, it is crucial to confirm the correct diagnosis as inflammatory demyelinating disease.

In the present study, we report two cases of tumor-like demyelinating lesions. Each case presented a large monofocal lesion, which was initially diagnosed as glioblastoma or low-grade glioma, but the pathologic findings demonstrated the inflammatory demyelinating process. The clinical features revealed the gradually progress of neurologic symptoms and signs, the improvement of the clinical and radiologic abnormalities following treatment with high-dose oral prednisolone, and the development of neither new symptoms nor lesions during the long follow-up period. Similar cases were previously described and termed tumor-like demyelinating lesions or monofocal acute inflammatory demyelination (MAID) [3–11].

Here, we discuss the clinical manifestations and pathophysiology of these cases together with a review of the relevant literature.

2. Case report

2.1. Case 1

In January 2003, a 53-year-old, right-handed Japanese male developed a visual field deficit and left hemiparesis. He consulted a local physician for the progress of hemiparesis over the course of 1 month. Radiologic analysis revealed the presence of a mass lesion, which was initially suspected to be a malignant glioma, and stereotactic biopsy of the mass was performed. Because the histologic diagnosis was consistent with inflammatory demyelinating disease, the patient was referred to our hospital for further evaluation. He had a history of diabetes mellitus and diabetic neuropathy. In addition, he had no history of preceding viral infection or immunization prior to the onset of his current symptoms. On admission, neurologic examination revealed homonymous hemianopsia, vertical gaze palsy, left hemifacial palsy, and moderate left hemiparesis, with the lower extremity being more severely affected. His deep reflexes were decreased, presumably due to diabetic neuropathy, but the left Chaddock sign was positive. Hypesthesia was noted on the left side of the body and extremities. Routine blood tests were normal. Analysis of the cerebrospinal fluid (CSF) showed the increase of total protein (139 mg/dl; normal < 40 mg/dl), and myelin basic protein (MBP) (224 pg/ml; normal < 102 pg/ml). The immunoglobulin (Ig) G in CSF

* Corresponding author. Tel.: +81 97 586 5814; fax: +81 97 586 6502.
E-mail address: noriyuki@med.oita-u.ac.jp (N. Kimura).

0303-8467/$ – see front matter © 2008 Elsevier B.V. All rights reserved.
doi:10.1016/j.clineuro.2008.10.010

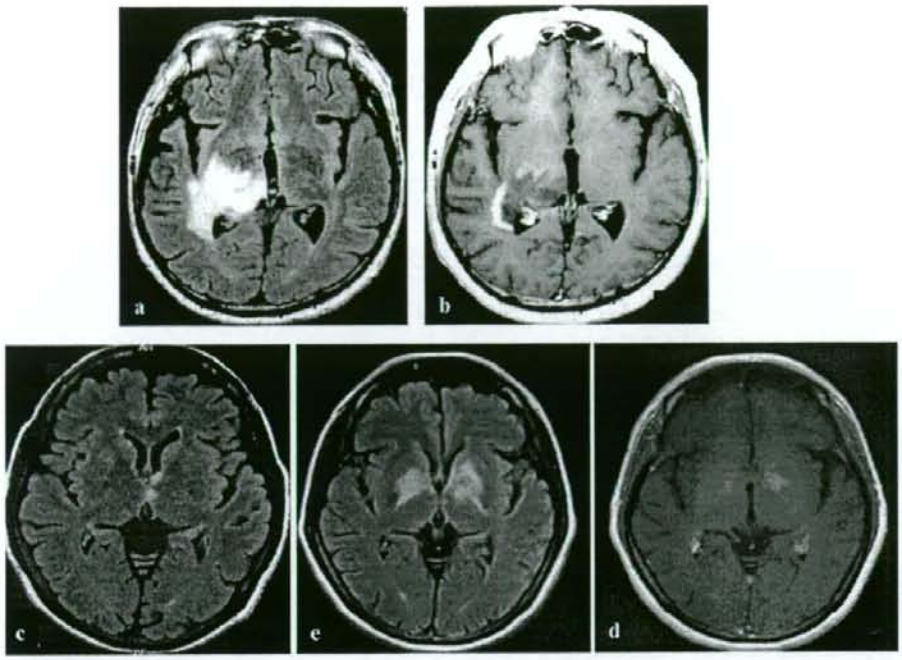

Fig. 1. Cranial MRI in case 1 (a and b) and case 2 (c–e). The right side is shown on the left-hand side of each figure. (a) Axial FLAIR image, obtained on admission, shows a large monofocal, hyperintense lesion with mild edema in the subependymal white matter of the right temporal lobe. (b) Axial gadolinium-enhanced T1-weighted image demonstrates open ring-like enhancement. (c) Axial FLAIR image, obtained at first examination, shows a small abnormal lesion in the left genu of the internal capsule and hypothalamus. (d) Follow-up axial FLAIR image, obtained on admission, shows a butterfly-shaped hyperintense lesion in the bilateral basal ganglia and the internal capsule without peripheral edema. (e) Axial gadolinium-enhanced T1-weighted image demonstrates focal contrast enhancement.

index was normal and oligoclonal bands were negative. Bacterial and fungal cultures were negative and no marked increase in antiviral titers in the serum or CSF was observed. Electroencephalogram (EEG) showed slow waves in the right temporal region. In March 2003, fluid-attenuated inversion recovery (FLAIR) MRI detected a large monofocal, hyperintense lesion. Gadolinium-enhanced MRI showed open ring-like enhancement in the subependymal white matter of right temporal lobe, which extended to the basal ganglia and midbrain (Fig. 1a and b). However, the peripheral edema and mass effect were disproportionately mild for the size of the lesion. MRI of the cervical, thoracic, or lumbar spine revealed no remarkable changes. The patient was treated with a high dose of oral prednisolone, 60 mg/day. Follow-up examination at 1 month revealed no abnormal neurologic symptoms. Two months later, repeated MRI revealed the absence of gadolinium enhancement and a decrease in the size of the periventricular lesion. He was discharged on a tapered dose of prednisolone and no relapse occurred during 5 years of follow-up.

2.2. Case 2

In December 2004, a 49-year-old, right-handed Japanese woman consulted a neurologist because of weakness in her right extremities over the preceding 2 weeks. Her medical and family history was unremarkable. Brain MRI showed a small abnormal lesion in the left genu of the internal capsule and the hypothalamus (Fig. 1c). Two months later, repeated MRI demonstrated that the lesion had extended to the ipsilateral lentiform nucleus and the contralateral basal ganglia through the anterior commissure. In mid-May, she was admitted to our hospital. On admission, the patient was drowsy and scored 10/30 on the Mini-Mental State examination (MMSE). She had mild weakness, rigidity, and hyperreflexia in the right extremities without pathologic reflex. Routine blood tests were normal. CSF analysis showed the increase of leukocyte count (39 mm^{-3}) and MBP level (124 pg/ml). EEG revealed diffuse slow waves. Repeated MRI demonstrated a butterfly-shaped lesion in the bilateral basal ganglia, characterized by a high-intensity signal on FLAIR images without edema and mass effect (Fig. 1d). Gadolinium-enhanced MRI showed focal contrast enhancement in the globus pallidus (Fig. 1e). She was initially treated with intravenous pulse methylprednisolone (1000 mg/day) for 3 days and high-dose oral prednisolone (60 mg/day). Although her CSF profiles returned to normal, cognitive impairment and right hemiparesis became worse over 1 month. Therefore, a butterfly glioma was suspected and a stereotactic brain biopsy was performed to verify the diagnosis. Histologic examination showed the inflammatory demyelinating lesion. High-dose oral prednisolone (60 mg/day) was continued and her neurologic symptoms gradually improved. Three months after initiation of the corticosteroid therapy, her neurologic symptoms returned to normal and MRI revealed the absence of gadolinium enhancement and a decrease in the size of the lesion. She was discharged on a tapered dose of prednisolone, and no relapse occurred during 2 years of follow-up.

2.3. Pathologic findings

The pathologic changes observed in case 1 (Fig. 2a–f) were more severe than those in case 2 (Fig. 2g and h), although both

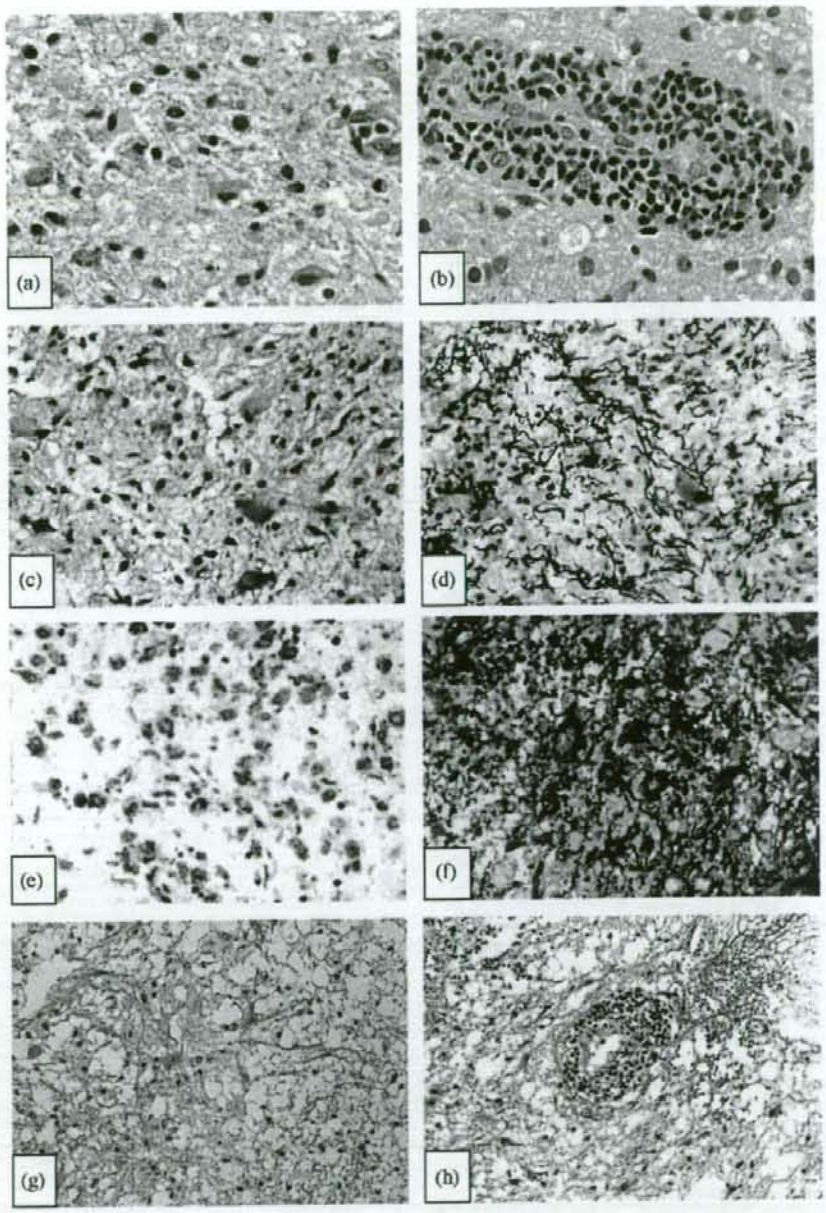

Fig. 2. Pathologic findings of the biopsy specimen obtained from case 1 (a–f) and case 2 (g–J). (a) Proliferation of numerous foamy macrophages and gemistocytic astrocytes (HE stain, 200×). (b) Massive perivascular lymphocyte cuffing (HE stain, 200×). (c) Severe myelin loss in areas infiltrated by macrophages, positive for myelin debris (Kluver–Barrera stain, 200×). (d) Relative preservation of axons in the lesion despite the myelin pallor (modified Bielschowsky stain, 200×). (e) Numerous foamy macrophages positive for CD 68 (200×). (f) Numerous gemistocytic astrocytes positive for GFAP (200×). (f) Proliferation of foamy macrophages and some reactive astrocytes (HE stain, 100×). (g) Moderate perivascular lymphocyte cuffing (HE stain, 100×).

cases shared marked morphologic similarities. The biopsy specimen was small and originated form the gadolinium-enhanced lesions. Hematoxylin and eosin (HE) staining revealed the severe tissue rarefaction with numerous foamy macrophages, and the intensive active gliosis with gemistocytic astrocytes proliferation throughout the lesions (Fig. 2a and g). Perivascular lymphocyte cuffing was observed at the periphery of the lesion, but there was no evidence of neovascularization (Fig. 2b and h). The characteristic

pathological findings of MS, such as the sharp border of the lesions and shadow plaques, could not be identified because of the near-total tissue rarefaction with diffuse infiltration of macrophages. Kluver–Barrera (KB) staining sowed severe myelin loss, and the broken-down myelin fragments in the cytoplasm of macrophage were observed (Fig. 2c). In contrast to the myelin pallor, modified Bielschowsky staining showed relatively well-preserved axons in the lesions (Fig. 2d). Numerous foamy macrophages were positive staining for CD68 (PMG1 monoclonal, diluted 1:200; Dako, Glostrup, Denmark) (Fig. 2e), and the gemistocytic astrocytes were positive staining for glial fibrillary acidic protein (GFAP, polyclonal; Dako, Denmark) within and around the lesion (Fig. 2f). Neither atypical cells nor any findings suggestive of a tumor was detected. These pathologic findings confirmed the diagnosis of active inflammatory demyelinating disease.

3. Discussion

We describe two cases with atypical clinical and MRI features of demyelinating lesions that resembled a glioblastoma and a butterfly shaped low-grade glioma. The present cases demonstrated the increase of protein level, MBP, or leukocyte count in CSF analysis and a large monofocal lesion with disproportionately mild or no peripheral edema or open ring-like enhancement on MRI, suggesting an ongoing inflammatory demyelinating process [2,12]. Stereotactic biopsy however was necessary to confirm the correct diagnosis because of the progressive clinical signs, initial unresponsiveness to corticosteroid treatment, and an actively growing lesion. The common pathologic findings of our cases were characterized by the severe myelin loss with relatively well-preserved axons, numerous foamy macrophages, proliferation of reactive astrocytes, and perivascular lymphocyte cuffing that are consistent with the inflammatory demyelinating plaque. Therefore, we speculate that the same immunologic mechanism participate in the development of these lesions, although the clinical and radiological findings were different.

In the previous reports, several demyelinating diseases, such as MS [13,14], acute disseminated encephalomyelitis (ADEM) [15], and myelinoclastic diffuse sclerosis (MDS) [16,17] sometimes presented with tumor-like lesions. MS is the most common form of primary demyelinating disease and the diagnosis largely depends on the clinical course, which is characterized by relapsing–remitting or progressive neurologic deficits. Unlike MS, ADEM is a monophasic inflammatory demyelinating disease, usually preceded by systemic viral infection or vaccination. Solitary or multiple lesions are distributed throughout the cerebral white matter, and frequently involve cortical and deep gray matter. MDS is a monophasic demyelinating disease that occurs mainly in children and demonstrates one or two symmetric bilateral lesions involving the centrum semiovale [16]. Our cases presented with no history of virus infection or vaccination, and monophasic clinical or radiologic deficits over long follow-up period. The monofocal lesion located in the right temporal white matter and bilateral basal ganglia without preference for periventricular area. Therefore, they did not clearly fit the diagnostic criteria for MS, ADEM, or MDS with regard to the clinical course and the location of lesions. In literature, similar cases were described and termed tumor-like demyelinating lesions or monofocal acute inflammatory demyelination (MAID) [3–11]. Clinical features of these cases show the acute onset of focal neurologic signs and normal CSF analysis except for the increase of protein or MBP levels in a few cases. Most of the cases demonstrated a good response to steroid therapy and monophasic episodes without relapse during long follow-up periods. The precise nosologic classification of these patients remains uncertain. Gutrecht et al. [7] suggested that MAID may be a unique form of acute, monofocal, cerebral demyelinating disease that appears to be more similar to ADEM than to MS. Moreover, some patients with MAID may have immunologic characteristics that prevent MS from developing. Poser et al. [2,16] considered tumor-like demyelinating lesions as variants of MS, whereas Kepes [1] suggested that they occupy an intermediate position between MS and ADEM. In our cases, the clinical course and radiologic findings favored ADEM except for no history of systemic viral infection or vaccination, lesion sizes however exceed that of the small foci of perivenous demyelination seen in typical ADEM. Moreover, pathologic features were consistent with those of the previous cases of tumor-like MS [13,14]. Therefore, present cases were similar to the published cases with tumor-like demyelinating lesions, which may represent an entity intermediate between MS and ADEM. We speculate that the same immunologic mechanisms may contribute to the pathogenesis of monofocal tumor-like demyelinating lesion.

In conclusion, we suggest that the inflammatory demyelinating disease should be considered, even if the patients with monofocal tumor-like lesions demonstrate the slowly progressive clinical course. Long term oral prednisolone therapy may be effective in these patients. Brain biopsy is a considered a diagnostic procedure for the correct diagnosis of tumor-like lesions and can contribute to the appropriate treatment.

References

[1] Kepes JJ. Large focal tumor-like demyelinating lesions of the brain: intermediate entity between multiple sclerosis and acute disseminated encephalomyelitis? A study of 31 patients. Ann Neurol 1993;33(1):18–27.
[2] Dagher AP, Smirniotopoulos J. Tumefactive demyelinating lesions. Neuroradiology 1996;38(6):560–5.
[3] Kalyan-Raman UP, Garwacki DJ, Elwood PW. Demyelinating disease of corpus callosum presenting as glioma on magnetic resonance scan: a case documented with pathological findings. Neurosurgery 1987;21(2):247–50.
[4] Censori B, Agostinis C, Partziguian T, Gazzaniga G, Biroli F, Mamoli A. Large demyelinating brain lesion mimicking a herniating tumor. Neurol Sci 2001;22(4):325–9.
[5] Heyman D, Delhaye M, Fournier D, Mercier P, Rousselet MC, Menei P. Pseudotumoral demyelination: a diagnosis pitfall (report of three cases). J Neurooncol 2001;54(1):71–6.
[6] Sugita Y, Terasaki M, Shigemori M, Sakata K, Morimatsu M. Acute focal demyelinating disease simulating brain tumors: histopathologic guidelines for an accurate diagnosis. Neuropathology 2001;21(1):25–31.
[7] Gutrecht JA, Berger JR, Jones Jr RH, Mancall AC. Monofocal acute inflammatory Demyelination (MAID): a unique disorder simulating brain neoplasm. South Med J 2002;95(1):1180–6.
[8] Tan HM, Chan LL, Chuah KL, Goh NS, Tang KK. Monophasic, solitary tumefactive demyelinating lesion: neuroimaging features and neuropathological diagnosis. Br J Radiol 2004;77(914):153–6.
[9] Mandrioli J, Ficarra G, Callari G, Sola P, Merelli E. Monofocal acute large demyelinating lesion mimicking brain glioma. Neurol Sci 2004;25:S386–8.
[10] Enzinger C, Strasser-Fuchs S, Ropele S, Kapeller P, Kleinert R, Fazekas F. Tumefactive demyelinating lesions: conventional and advanced magnetic resonance imaging. Mult Scler 2005;11(2):135–9.
[11] Akimoto J, Nakajima N, Saida A, Haraoka J, Kudo M. Monofocal acute inflammatory demyelination manifesting as open ring sign. Case report. Neurol Med Chir (Tokyo) 2006;46(7):353–7.
[12] Masdeu JC, Quinto C, Olivera C, Tenner M, Leslie D, Visintainer P. Open-ring imaging sign: highly specific for atypical brain demyelination. Neurology 2000;54(7):1427–33.
[13] Nesbit GM, Forbes GS, Scheithauer BW, Okazaki H, Rodriguez M. Multiple sclerosis: histopathologic and MR and/or CT correlation in 37 cases at biopsy and three cases at autopsy. Radiology 1991;180(2):467–74.
[14] Di Patre PL, Castillo V, Delavelle J, Vuillemoz S, Picard F, Landis T. "Tumor-mimicking" multiple sclerosis. Clin Neuropathol 2003;22(5):235–9.
[15] Singh S, Alexander M, Sase N, Korah IP. Solitary hemispheric demyelination in acute disseminated encephalomyelitis: clinicoradiological correlation. Australas Radiol 2003;47(1):29–36.
[16] Poser CM, Goutières F, Carpentier MA, Aicardi J, Schilder's myelinoclastic diffuse sclerosis. Pediatrics 1986;77(1):107–12.
[17] Afifi AK, Bell WE, Menezes AH, Moore SA. Myelinoclastic diffuse sclerosis (Schilder's disease): report of a case and review of the literature. J Child Neurol 1994;9(4):398–403.

ELSEVIER

Journal of the Neurological Sciences 269 (2008) 163–168

Journal of the Neurological Sciences

www.elsevier.com/locate/jns

Short communication

Corticobasal degeneration presenting with progressive conduction aphasia

Noriyuki Kimura *, Toshihide Kumamoto, Takuya Hanaoka, Yusuke Hazama, Kenichiro Nakamura, Ryuki Arakawa

Department of Neurology and Neuromuscular Disorders, Oita University, Faculty of Medicine, Oita, Japan

Received 25 July 2007; received in revised form 5 December 2007; accepted 6 December 2007
Available online 29 January 2008

Abstract

We report the case of a woman with primary progressive aphasia (PPA) presenting with conduction aphasia. Neurological findings showed bilateral finger tremor and *signe de poignet figé* in her right hand. Memory, orientation, and activities of daily living were well preserved. Linguistic examination showed severe impairment in repetition, fluent spontaneous speech with phonemic paraphasia, and relatively well preserved comprehension. Limb-kinetic apraxia and parkinsonism were not observed during the course of her illness. T1-weighted magnetic resonance imaging revealed severe atrophy of the left temporal lobe and dilatation of the left Sylvian fissure. Neuropathological findings demonstrated the most severe atrophy in the left superior temporal gyrus and Gallyas–Braak-positive or phosphorylated tau-immunoreactive cytoskeletal structures, which were consistent with corticobasal degeneration (CBD). We speculate that the progressive conduction aphasia of our patient might have been caused by left temporal lobe impairment. We suggest that progressive conduction aphasia may be a feature of CBD presenting with PPA.

Keywords: Corticobasal degeneration; Primary progressive aphasia; Conduction aphasia; Abnormal cytoskeletal structures; Left superior temporal gyrus

1. Introduction

In 1982, Mesulam described six patients who experienced language disorders that progressed slowly over many years [1]; he subsequently named this condition primary progressive aphasia (PPA) [2]. Primary progressive aphasia is a clinical syndrome characterized by slowly progressive loss of speech and language function in the setting of relatively preserved memory and visuospatial skills within the initial two years [2,3]. Recent studies have indicated that PPA is clinically and histopathologically heterogeneous, and several underlying pathologies have been described, such as Alzheimer's disease [4], Pick's disease [5], Pick complex [6], non-specific cortical degeneration with spongiform change or dementia lacking distinct histology [7], Creutzfeldt–Jakob disease [8], corticobasal degeneration (CBD) [9–16], and motor neuron disease with dementia [17].

Here, we reported the rare case of a patient with PPA presenting with conduction aphasia of the fluent type. Although our patient did not show the typical symptoms of CBD at any time during the course of the disease, the post-mortem examination confirmed a diagnosis of CBD. Conduction aphasia is characterized by markedly impaired repetition of words and phrases with normal or nearly normal comprehension and was originally proposed to result from a separation of the posterior language comprehension area and the anterior motor speech area of the left hemisphere [18]. Such a disconnection has been attributed to a lesion of the arcuate fasciculus [19]. The neuropathological findings of our patient revealed that cerebral involvement was accentuated in the left superior temporal gyrus and various types of cytoskeletal abnormalities were observed in the cerebral cortex and white matter, mainly in the frontal lobe, as well as

* Corresponding author. Department of Neurology and Neuromuscular Disorders, Oita University, Faculty of Medicine, Idaigaoka 1-1, Hasama, Yufu, Oita 879-5593, Japan. Tel.: +81 97 586 5814; fax: +81 97 586 6502.
E-mail address: noriyuki@med.oita-u.ac.jp (N. Kimura).

0022-510X/$ - see front matter © 2007 Elsevier B.V. All rights reserved.
doi:10.1016/j.jns.2007.12.017

in the basal ganglia and brainstem. To our knowledge, this is the first report of an autopsy case of CBD with progressive conduction aphasia. In this report, we focus on the relationship between cortical foci of degenerating areas and the clinical expression of CBD.

2. Case report

The patient was a right-handed woman who had graduated from high school. There was no family history of neurological problems. At the age of 67 years, she became aware of a speech disturbance, specifically phonemic paraphasia in her spontaneous speech. Although she could perform household activities and her daily routine by herself, and her personality did not change, her language abilities gradually deteriorated. At the age of 69 years, she visited our hospital with language problems.

On neurological examination, she appeared alert and oriented. There were no abnormalities of the cranial nerves, muscle strength, deep tendon reflexes, or sensory system, except for mild upward gaze limitation. She showed bilateral hand-finger tremor and *signe de poignet figé* in her right hand, but neither bradykinesia, gait disturbance, nor Myerson's sign. On neuropsychological study, the Mini-Mental State Examination (MMSE) was within the normal range, at 23 points. The Wechsler Adult Intelligence Scale-Revised (WAIS-R) was abnormal, at 61 points, because the verbal intelligence quotient (60) was low for aphasia, despite a normal performance intelligence quotient (82). Apraxia, agnosia, and dyscalculia were absent. The standard language test of aphasia revealed that spontaneous speech was fluent, but phonemic and verbal paraphasia were obvious on naming, reading aloud, and repetition. She was unable to repeat short sentences. She recognized her own errors and tried hard to correct them by herself. Impairment of repetition was the most prominent of the linguistic abnormalities. Her writing was slightly disturbed in both kana and kanji. By contrast, her auditory comprehension was normal. The profile of her language impairment was consistent with that of conduction aphasia.

Her routine blood tests, electrocardiography, and electroencephalography were normal. Cranial T1-weighted magnetic resonance images (MRI) revealed severe atrophy of the left temporal lobe and dilatation of the left Sylvian fissure (Fig. 1a, b). Tc-99m-hexamethylpropyleneamine oxine single photon emission computed tomography (SPECT; GCA9300A/HG, Toshiba, Tokyo, Japan) showed mild hypoperfusion in the left temporal and parietal lobes (Fig. 1c).

Three years after the onset of this condition, memory, orientation, and activities of daily living were well preserved, but linguistic disturbance had progressed. Neuropsychological reevaluation demonstrated that language fluency, auditory comprehension, writing, and reading were mild impaired, in contrast to a severe disturbance in repetition. Limb-kinetic apraxia and Parkinsonian symptoms were not observed during the course of her illness. The follow-up MRI showed that the atrophy of left temporal lobe was slightly progressed. She died of lung cancer at the age of 72 years, 5 years after the onset of symptoms. The clinical diagnosis was PPA.

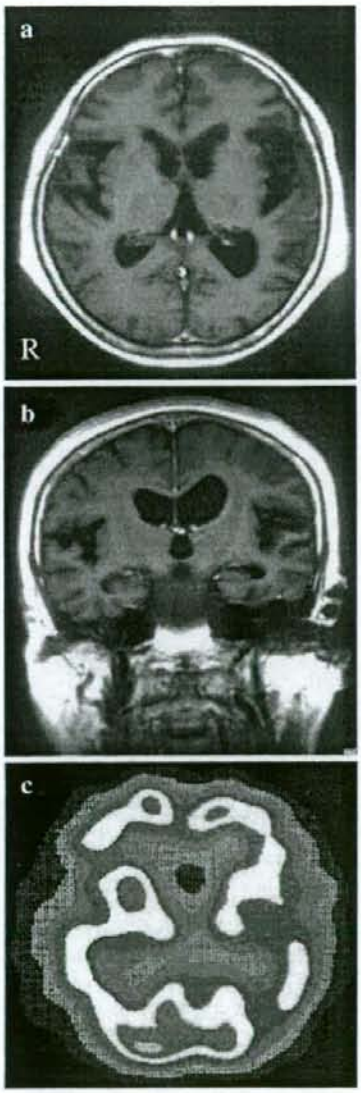

Fig. 1. T1-weighted MRI and 123I-IMP-SPECT images. T1-weighted MRI revealed severe atrophy of the left temporal lobe and dilation of the left Sylvian fissure (a, b). Hypoperfusion was noted in the left perisylvian area (c). The right side is shown on the left-hand side of each figure.

2.1. Post-mortem examination

The brain weight was 1170 g after fixation. Macroscopic examination revealed slight atrophy in the frontal and temporal lobes, more accentuated on the left side. The most severe atrophy was found in the left superior temporal gyrus, especially the anterior portion (Fig. 2a). The left Sylvian fissure was moderately dilated. The parietal and occipital lobes showed normal convolutions. Coronal slices disclosed moderate to mild atrophy of the caudate nucleus, putamen, and globus pallidus, slightly accentuated on the left side (Fig. 2b). The substantia nigra was pale (Fig. 2c).

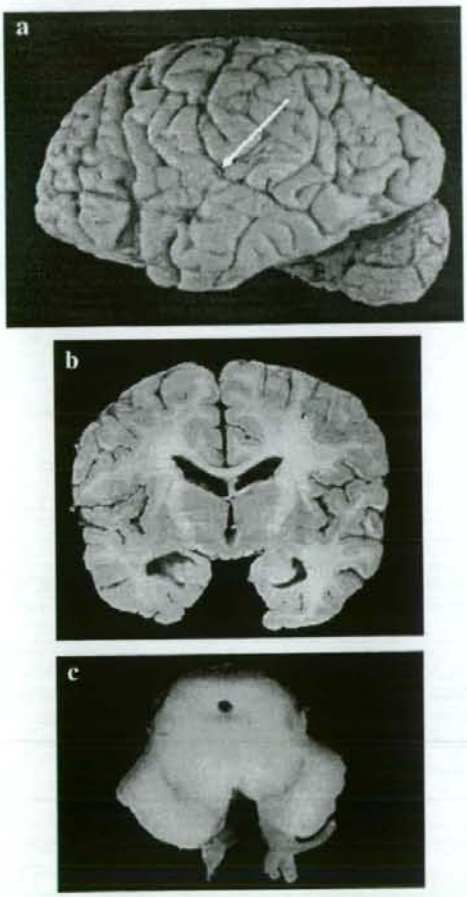

Fig. 2. Lateral view of the left cerebrum exhibits atrophy of the superior temporal gyrus and slight enlargement of the left Sylvian fissure (a). Coronal section of the brain at the mammillary body level shows marked atrophy of the left superior temporal gyrus and slight atrophy of the caudate, putamen, globus pallidus, and thalamus on the left side (b). Transverse section of the midbrain shows marked depigmentation of the substantia nigra (c).

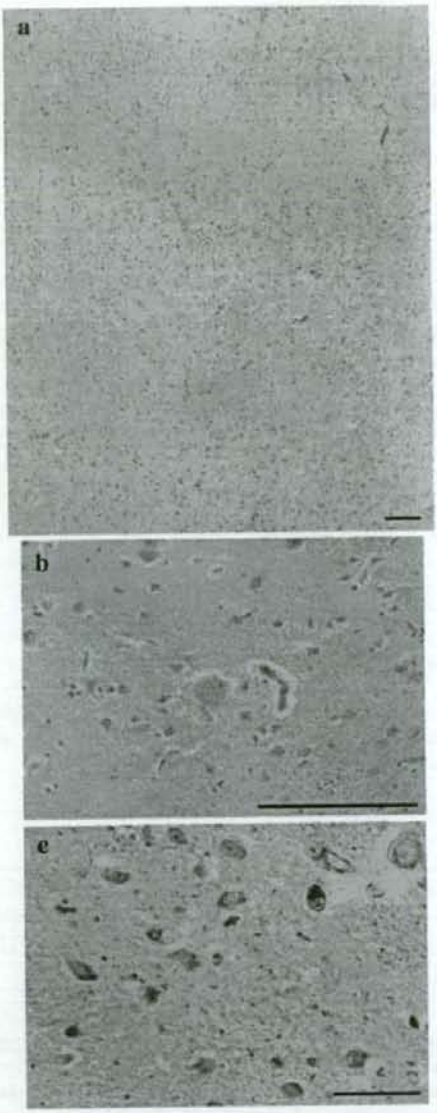

Fig. 3. In the superior temporal cortex, all layers show neuronal loss and gliosis (a). Ballooned neurons are seen in the frontal cortex (b). Moderate neuronal loss and extraneuronal pigment are present in the substantia nigra (c). Hematoxylin and eosin stain. Scale bars 100 μm.

Histological examination demonstrated moderate neuronal loss with gliosis (Fig. 3a) and a spongy appearance throughout all layers of the left superior temporal gyrus. The frontal, parietal, and occipital lobes and the remainder of the temporal lobe were relatively well preserved. Numerous ballooned neurons were seen in the frontal cortex and occasionally in the temporal, parietal, and occipital cortices

(Fig. 3b). Diffuse fibrillary gliosis was observed in the white matter with a distribution corresponding to cortical degeneration. Neuronal loss and gliosis were moderate in the substantia nigra and mild in the striatum and globus pallidus. There were no Lewy bodies in the cerebrum and brainstem. With modified Bielschowsky staining, Pick bodies and senile plaques were not seen in the cerebral cortex or hippocampus. A few neurofibrillary tangles were present in the CA1 region of the hippocampus. Grumose degeneration was also present in the dentate nucleus. The modified Gallyas–Braak staining and anti-phosphorylated tau immunostaining revealed massive argyrophilic and anti-phosphorylated tau-positive threads, scattered coiled bodies, pretangles, and astrocytic plaques in the neurons and glial cells (Fig. 4a–c). Pretangles and astrocytic plaques were found mainly in the frontal cortex, in spite of mild neuronal loss and gliosis. However, these cytoskeletal abnormalities were observed less frequently in the severely affected left superior temporal gyrus. The argyrophilic threads were most prominent in the affected cortical region, but they were also observed in the relatively well preserved cortex, basal ganglia, and brainstem. In addition, numerous argyrophilic threads and coiled bodies were also seen in the white matter of the cerebrum, cerebellum, and brainstem.

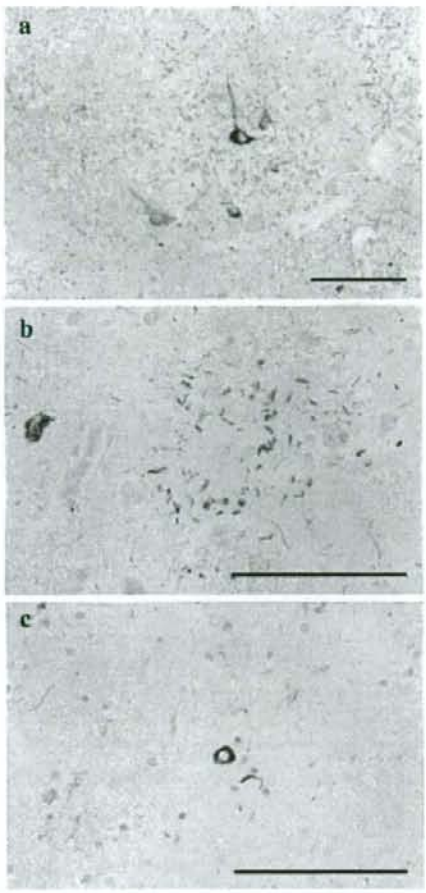

Fig. 4. Phosphorylated tau immunohistochemistry showed diffuse or granular staining of neurons (pretangles) and threads throughout the frontal cortex (a). An astrocytic plaque is seen in the cortex (b). A phosphorylated tau-positive inclusion in a glial cell in the white matter. (c). Phosphorylated tau immunohistochemistry. Scale bars 100 μm.

3. Discussion

We described a case of CBD with slowly progressive language disorder without dementia, parkinsonism, and pyramidal signs. The patient was able to manage her household during the course of her illness and was clinically deemed to have typical PPA. The clinical representations of PPA are sub-divided into fluent and non-fluent forms [20]. Fluent forms are characterized by impairment of auditory comprehension and empty, circumlocutory speech. Non-fluent forms are associated with stuttering or dysprosodic speech, articulatory disturbances, and agrammatism. In the present case, linguistic examination showed severe impairment of repetition, fluent spontaneous speech with phonemic paraphasia, and relatively well preserved comprehension. Conduction aphasia is characterized by fluency and paraphasia in spontaneous speech, with normal or nearly normal comprehension of spoken language but markedly impaired repetition of words and phrases [18]. The patient's condition was therefore diagnosed as PPA presenting with conduction aphasia.

Although the clinical symptoms of our patient were unusual, post-mortem examination showed pathological features of CBD. Corticobasal degeneration has been recognized as one type of disorder presenting with PPA [9–16]. Clinically, CBD is characterized by an asymmetric, akinetic, rigid syndrome with prominent apraxia, myoclonus, cortical sensory loss, and sometimes alien limb behavior [21]. The occurrence of aphasia and dementia has not been recognized in CBD for a long time; however, autopsy-confirmed cases of CBD have revealed that cognitive impairment and speech problems are prominent clinical features of the disease. Graham et al. reported that 34% of patients with pathological confirmation were noted to be aphasic [22].

Neuropathologically, CBD is characterized by asymmetric atrophy of the frontal and parietal lobes, swollen achromatic neurons, and degeneration of the substantia nigra. Recent neuropathological criteria emphasize Gallyas–Braak-positive or tau-immunoreactive lesions such as pretangles, astrocytic plaques, coiled bodies, and argyrophilic threads in neurons and glia [23]. Neuropathological examination of our patient revealed marked atrophy with neuronal loss and gliosis in the left superior temporal gyrus and substantia nigra, and to a lesser extent, the striatum, globus pallidus, and brainstem. Gallyas–Braak-positive or

tau-immunoreactive cytoskeletal structures were observed in the cortical and sub-cortical regions, mainly in the frontal lobe. These neuropathological findings were consistent with the recent neuropathological criteria of CBD [24].

Only eight pathologically confirmed cases of CBD with PPA have been reported (Table 1) [9–16]. According to these reports, non-fluent aphasia was observed in five cases, whereas three cases showed the fluent form. All cases with non-fluent aphasia revealed a marked atrophy in the left superior or inferior frontal gyrus, while two of three cases with fluent aphasia showed marked atrophy in the left superior temporal gyrus. The present case with fluent aphasia also showed the most severe atrophy in the left superior temporal gyrus. We suggest that the fluent type of PPA may be caused by a lesion of the left superior temporal gyrus.

The cardinal symptoms of conduction aphasia are significant impairments in word repetition with preserved comprehension, naming, and reading. Wernicke postulated that any lesion disrupting the arcuate fasciculus should result in conduction aphasia. The arcuate fasciculus is a white matter tract from the site of auditory language comprehension to the site of motor expression of speech [19]. By contrast, Goldstein attributed conduction aphasia to a disturbance of a localized cortical center [25]. He suggested that the linguistic mechanisms of conduction aphasia were due to a disturbance of verbal short-term memory and phonological output. The lesions might be in the inferior parietal lobe, especially the supramarginal gyrus, and the superior temporal gyrus [26–28]. These results suggest that conduction aphasia may be a heterogeneous syndrome anatomically and linguistically. We speculate that the progressive conduction aphasia of our patient might have been caused by a disturbance of short-term memory due to a lesion in the left superior temporal gyrus. In addition, a previous report of a case of PPA presenting with conduction aphasia revealed atrophy of the left superior temporal gyrus, although this was not pathologically confirmed [29]. Thus, the present case suggests that conduction aphasia might be caused by an impairment of the left superior temporal gyrus in the present case. Further studies are needed to clarify the correlation between pathological lesions and the aphasic form of CBD with progressive conduction aphasia.

In summary, we reported the first case of CBD with progressive conduction aphasia. The neuropathological findings of our case showed severe atrophy of the left superior temporal gyrus. This case is important for understanding the clinical heterogeneity and clinicopathological correlation of CBD with progressive conduction aphasia.

Table 1
Aphasic form and most severely affected site in eight previously reported cases and the present case of corticobasal degeneration with primary progressive aphasia

Author (year)	Age at onset	Aphasic form	Most affected cortical region
Lippa et al. (1990)	72/M	Non-fluent	Left parasylvian
Lippa et al. (1991)	68/M	Transcortical motor (non-fluent)	Left superior frontal gyrus
Arima et al. (1994)	73/M	Amnesic (fluent)	Left superior temporal gyrus
Sakurai et al. (1996)	72/M	Amnesic (fluent)	Right frontal
Ikeda et al. (1996)	67/F	Sensory (fluent)	Left superior temporal gyrus
Mimura et al. (2001)	65/F	Transcortical motor (non-fluent)	Left inferior frontal gyrus
Sánchez et al. (2006)	57/F	Non-fluent	Left frontal operculmus and pre-motor area
Takao et al. (2006)	67/F	Non-fluent	Left inferior frontal gyrus
Present case (2007)	67/F	Conduction (fluent)	Left superior temporal gyrus

References

[1] Mesulam MM. Slowly progressive aphasia without generalized dementia. Ann Neurol 1982;11:592–8.
[2] Mesulam MM. Primary progressive aphasia. Ann Neurol 2001;49:425–32.
[3] Kertesz A, Hudson L, Mackenzie IR, Munoz DG. The pathology and nosology of primary progressive aphasia. Neurology 1994;44:2065–72.
[4] Greene JD, Hodges JR, Ironside JW, Warlow CP. Alzheimer disease and nonfluent progressive aphasia. Arch Neurol 1996;53:1072–8.
[5] Graff-Radford NR, Damasio AR, Hyman BT, Hart MN, Tranel D, Damasio H, et al. Progressive aphasia in a patient with Pick's disease: a neuropsychological, radiologic, and anatomic study. Neurology 1990;40:620–6.
[6] Kertesz A, Munoz DG. Primary progressive aphasia. Clin Neurosci 1997;4:95–102.
[7] Kirshner HS, Tanridag O, Thurman L, Whetsell Jr WO. Progressive aphasia without dementia: two cases with focal spongiform degeneration. Ann Neurol 1987;22:527–32.
[8] Mandell AM, Alexander MP, Carpenter S. Creutzfeldt–Jakob disease presenting as isolated aphasia. Neurology 1989;39:55–8.
[9] Ikeda K, Akiyama H, Iritani S, Kase K, Arai T, Niizato K, et al. Corticobasal degeneration with primary progressive aphasia and accentuated cortical lesion in superior temporal gyrus: case report and review. Acta Neuropathol 1996;92:534–9.
[10] Takao M, Tsuchiya K, Mimura M, Momoshima S, Kondo H, Akiyama H, et al. Corticobasal degeneration as cause of progressive non-fluent aphasia: clinical, radiological and pathological study of an autopsy case. Neuropathology 2006;26:569–78.
[11] Sanchez-Valle R, Forman MS, Miller BL, Gorno-Tempini ML. From progressive nonfluent aphasia to corticobasal syndrome: a case report of corticobasal degeneration. Neurocase 2006;12:355–9.
[12] Mimura M, Oda T, Tsuchiya K, Kato M, Ikeda K, Hori K, et al. Corticobasal degeneration presenting with nonfluent primary progressive aphasia: a clinicopathological study. J Neurol Sci 2001;183:19–26.
[13] Sakurai Y, Hashida H, Uesugi H, Arima K, Murayama S, Bando M, et al. A clinical profile of corticobasal degeneration presenting as primary progressive aphasia. Eur Neurol 1996;36:134–7.
[14] Lippa CF, Smith TW, Fontneau N. Corticonigral degeneration with neuronal achromasia. A clinicopathologic study of two cases. J Neurol Sci 1990;98:301–10.
[15] Lippa CF, Cohen R, Smith TW, Drachman DA. Primary progressive aphasia with focal neuronal achromasia. Neurology 1991;41:882–6.
[16] Arima K, Uesugi H, Fujita I, Sakurai Y, Oyanagi S, Andoh S, et al. Corticonigral degeneration with neuronal achromasia presenting with primary progressive aphasia: ultrastructural and immunocytochemical studies. J Neurol Sci 1994 20;127:186–97.

[17] Mitsuyama Y. Presenile dementia with motor neuron disease in Japan: clinico-pathological review of 26 cases. J Neurol Neurosurg Psychiatry 1984;47:953–9.
[18] Bartha L, Benke T. Acute conduction aphasia: an analysis of 20 cases. Brain and Lang 2003;85(1):93–108.
[19] Damasio H, Damasio AR. The anatomical basis of conduction aphasia. Brain 1980;103:337–50.
[20] Rosen HJ, Kramer JH, Gorno-Tempini ML, Schuff N, Weiner M, Miller BL. Patterns of cerebral atrophy in primary progressive aphasia. Am J Geriatr Psychiatry 2002;10:89–97.
[21] Rebeiz JJ, Kolodny EH, Richardson Jr EP. Corticodentatonigral degeneration with neuronal achromasia. Arch Neurol 1968;18:20–33.
[22] Graham NL, Bak TH, Hodges JR. Corticobasal degeneration as a cognitive disorder. Mov Disord 2003;18:1224–32.
[23] Ferrer I, Hernandez I, Boada M, Llorente A, Rey MJ, Cardozo A, et al. Primary progressive aphasia as the initial manifestation of corticobasal degeneration and unusual tauopathies. Acta Neuropathol 2003;106:419–35.
[24] Dickson DW, Bergeron C, Chin SS, Duyckaerts C, Horoupian D, Ikeda K, et al. Office of Rare Diseases of the National Institutes of Health. Office of Rare Diseases neuropathologic criteria for corticobasal degeneration. J Neuropathol Exp Neurol 2002;61:935–46.
[25] Goldstein K. Language and language disturbance. New York: Grune & Stratton Inc.; 1948.
[26] Axer H, von Keyserlingk AG, Berks G, von Keyserlingk DG. Supra- and infrasylvian conduction aphasia. Brain Lang 2001;76:317–31.
[27] Quigg M, Fountain NB. Conduction aphasia elicited by stimulation of the left posterior superior temporal gyrus. J Neurol Neurosurg Psychiatry 1999;66:393–6.
[28] Anderson JM, Gilmore R, Roper S, Crosson B, Bauer RM, Nadeau S, et al. Conduction aphasia and the arcuate fasciculus: A reexamination of the Wernicke–Geschwind model. Brain Lang 1999;70:1–12.
[29] Hachisuka K, Uchida M, Nozaki Y, Hashiguchi S, Sasaki M. Primary progressive aphasia presenting as conduction aphasia. J Neurol Sci 1999;167:137–41.

Neuropathology 2008; **28**, 627–632 doi:10.1111/j.1440-1789.2008.00898.x

Case Report

Portal-systemic shunt encephalopathy presenting with diffuse cerebral white matter lesion: An autopsy case

Noriyuki Kimura, Toshihide Kumamoto, Takuya Hanaoka, Kenichiro Nakamura, Yusuke Hazama and Ryuki Arakawa

Department of Neurology and Neuromuscular Disorders, Oita University, Faculty of Medicine, Oita, Japan

We report herein an autopsy case of portal-systemic encephalopathy (PSE) presenting with diffuse tissue rarefaction in the cerebral deep white matter. Clinically, the patient showed recurrent episodes of unconsciousness, abnormal behavior and urinary incontinence, as well as flapping tremor. Cognitive impairment and peripheral neuropathy developed following recurrent episodes. Although conventional arterial portography revealed a small portal-systemic collateral vessel of a left gastro-renal venous shunt, abdominal CT and liver biopsy showed no evidence of liver cirrhosis and serum ammonia level showed a mild increase. T2-weighted MRI demonstrated symmetrical signal hyperintensities in the deep white matter. Neuropathological findings showed Alzheimer type II astrocytes in the deep layers of the cerebral cortices and severe tissue rarefaction with no or slight reactive astrocytosis in the subcortical and deep white matter. These white matter changes have been reported infrequently in patients with PSE. The present case suggests that chronic PSE without liver cirrhosis may develop diffuse white matter lesions.

Key words: Alzheimer type II astrocyte, diffuse white matter lesion, gastro-renal shunt, peripheral nerupathy, portal-systemic encephalopathy.

INTRODUCTION

Portal-systemic shunt occurs due to liver cirrhosis or idiopathic portal hypertension, and plays an important role in the etiology of recurrent hepatic encephalopathy.[1] In the 1950s, Sherlock *et al.* and White *et al.* emphasized the pathophysiological role of ammonia, which is generated in the intestine and flows directly into the systemic circulation through shunt vessels.[2,3] This syndrome is thus referred to as portal-systemic encephalopathy (PSE) or Inose's type hepatocerebral degeneration.[4] In general, PSE is clinically characterized by recurrent episodes of disturbed consciousness and other neurological symptoms such as flapping tremor of the outstretched hands, extrapyramidal symptoms, and hyper-reflexia during the non-episodic period.[5,6] Hyperintensity in bilateral lenticular nuclei on T1-weighted MRI is the characteristic finding of PSE.[7] Neuropathological findings show Alzheimer type II cells and spongiform changes in the gray matter.[8] Some investigators have recently claimed to have observed PSE in patients without liver cirrhosis or portal hypertension.[9–12] Although clinical and radiological findings were well described, neuropathological examinations of brain tissue from autopsy were limited in those cases.

We encountered an autopsy case of PSE due to congenital gastro-renal shunt without liver cirrhosis and portal hypertension. The patient had experienced recurrent episodes of unconsciousness accompanied by peripheral neuropathy and dementia. Interestingly, pathological findings showed diffuse tissue rarefaction due to severe loss of myelin and axons in the cerebral deep white matter, in addition to Alzheimer type II astrocytes in the cerebral cortex. Although some reports have described diffuse white matter lesions in hepatic encephalopathy, such changes are rare in PSE. We therefore describe the clinico-neuropathological findings of this patient with PSE, and discuss the correlations between MRI and pathological findings.

Correspondence: Noriyuki Kimura, MD, Department of Neurology and Neuromuscular Disorders, Oita University, Faculty of Medicine, Idaigaoka 1-1, Hasama, Yufu, Oita 879-5593, Japan. Email: noriyuki@med.oita-u.ac.jp

Received 5 December 2007; revised 9 January 2008 and accepted 10 January 2008.

CLINICAL SUMMARY

A 61-year-old Japanese woman developed fever, pain in the upper extremity and confusional state, despite good health until November 1993. Symptoms lasted for 24 h, and then subsided without treatment. She had experienced the same episodes twice before admission. Episodes would vary in duration from 24 h to 2 weeks and did not correlate with dietary changes or any other specific factors. She was admitted to our hospital on April 24, 1996, due to recurrent episodes of disturbed consciousness, abnormal behavior and urinary incontinence. No history of alcohol or drug abuse or significant family history could be elicited. On admission, no signs of liver disease were apparent such as jaundice, hepatosplenomegaly or vascular spider, with the exception of mild palmar erythema. Neurological examination showed drowsy state, disorientation and abnormal behavior such as restlessness and loud crying. Cranial nerve signs and muscle strength were normal, but muscle tone and deep reflexes were decreased. Flapping tremor of bilateral hands appeared occasionally. She displayed severe painful paresthesia in the extremities. No other neurological signs were identified, such as dysarthria, incoordination or extrapyramidal signs.

Laboratory findings revealed normal blood count and mild liver dysfunction as follows: aspartate aminotransferase, 211 IU/L (normal, 13–33 IU/L); alanine aminotransferase, 257 IU/L (normal, 6–27 IU/L); γ-glutamyl transferase, 113 IU/L (normal, 10–47 IU/L). Serum ammonia level was mildly increased at 42 μmol/L (normal, 9–33 μmol/L). Molar ratio of branched-chain amino acids (leucine, isoleucine and valine) to aromatic amino acids (tyrosine and phenylalanine) had decreased to 2.25 (normal, 2.43–4.40). An indocyanine green test showed 15% retention at 15 min (normal, <10%). Serum copper and ceruloplasmin levels were normal. Hepatitis B surface antigen and antibody were both negative, as was a test for hepatitis C virus antibody. A test for antinuclear antibody was positive, but antimitochondrial antibody and antismooth muscle antibodies were negative. Serum and urinary amino acid analyses yielded normal results. Specific patterns of aminograms as in citrullinaemia and argininosuccinic aciduria, which usually accompany hyperammonaemia, were not identified. White blood lysosome enzyme assay showed normal results. Blood levels of very-long-chain fatty acids were within normal limits. Analysis of CSF was unremarkable for cells, protein and glucose. EEG showed a diffuse θ wave, but not triphasic waves. Brain MRI demonstrated symmetrical signal hyperintensities in the deep cerebral white matter on T2-weighted imaging, but no signal abnormalities in bilateral basal ganglia on T1-weighted imaging (Fig. 1a,b). Sonography and CT of the abdomen showed no abnormalities, including shunt vessels. Endoscopic examination did not reveal esophageal or gastric varices or *Helicobacter pylori* infection. Ultrasound-guided fine needle liver biopsy showed mild lymphocytic infiltration without fibrosis in the portal tracts, indicating autoimmune hepatitis without liver cirrhosis. Conventional arterial portography disclosed a small portal-systemic collateral vessel of a left gastro-renal venous shunt (Fig. 1c). However, both the radiologist and gastroenterologist excluded the contribution of the shunt to recurrent episodes of unconsciousness because the size of the shunt vessel was insufficient to result in encephalopathy. Therefore the diagnosis of PSE could not be confirmed, and the hyperammonaemia might occur due to unknown causes. Conservative treatments such as administration of lactulose and infusion of branched-chain amino acid-enriched solution were performed for normalization of blood ammonia levels. The patient became free from episodes of loss of consciousness after several days of these treatments and was discharged on July 17.

The patient was subsequently admitted to our hospital with similar episodes twice over the next 3 years. Although neurological symptoms and laboratory data were almost the same as on first admission, cognitive function deteriorated (Mini-Mental State Examination, 21 points; revised Wechsler Adult Intelligence Scale, 80 points). In addition, a nerve conduction study revealed reduced conduction velocity of motor and sensory nerves in all extremities. Pathological findings of sural nerve biopsy revealed segmental demyelination and myelinated fiber loss without vascular inflammation (Fig. 2h). A density of the myelinated fibers revealed a decrease number of both large-diameter and small-diameter fibers. Teased-fiber analysis showed 53% were normal fibers, 43% had segmental demyelination and segmental remyelination, 1% had axonal degeneration, and 3% were unclassifiable.

Follow-up MRI demonstrated that cerebral white matter lesions extended from deep to subcortical white matter. Disturbance of consciousness was also improved for a few days with antihyperammonaemia therapy, but neurological symptoms including cognitive impairment continued to worsen and the patient died of pulmonary embolism in November 2001. Total duration from onset of the first episode to death was 8 years.

PATHOLOGICAL FINDINGS

Macroscopic findings

The brain, weighing 1100 g after fixation, showed slight cerebral atrophy. Coronal sections revealed moderate atrophy of cerebral white matter with dilatation of the lateral ventricle. Tissue softening was observed diffusely in the white matter. Multiple small lesions with greyish dis-

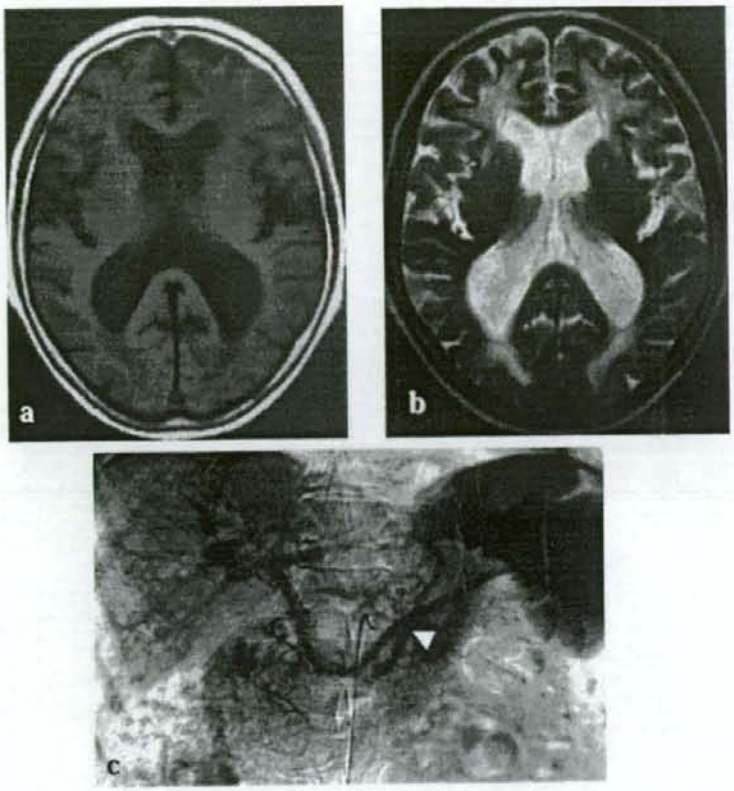

Fig. 1 T1- and T2-weighted MRI and conventional arterial portography. (a) T1-weighted MRI shows no abnormal signals in bilateral basal ganglia. (b) T2-weighted MRI shows diffuse signal hyperintensities in the deep cerebral white matter. (The right side is shown on the left-hand side of each figure). (c) Conventional arterial portography revealed small portal-systemic collateral vessel of a left gastro-renal venous shunt (arrowhead).

coloration were scattered in the subcortical white matter (Fig. 2a). Deep white matter revealed diffuse greyish discoloration. The cerebral cortex, subcortical gray matter, brainstem and cerebellum appeared normal.

Microscopic findings

Histological examinations were performed using HE, KB and Bielschowsky stains and immunohistochemical methods. HE staining revealed slight dilatation of perivascular and perineuronal spaces in the deep layer of the cerebral cortex (Fig. 2b), multiple focal tissue rarefaction in the subcortical white matter, and diffuse tissue rarefaction in the deep white matter (Fig. 2c). Bilateral putamina, globus pallidi, caudate nuclei and thalami were well preserved. There were Alzheimer type II astrocytes (Fig. 2d), which showed large, pale nuclei with marginated chromatin and scanty cytoplasm, some in the cerebral cortices, globus pallidus, and thalamus, a few in the putamen, caudate nucleus, and claustrum. No Alzheimer type I glial cells or Opalski's cells were present. KB and Bielschowsky staining revealed severe myelin pallor and axonal loss in the subcortical and deep white matter, including the U-fiber area (Fig. 2e,f). Subcortical white matter lesions were small and distributed in multiple regions, whereas deep white matter lesions were most severe and diffusely extended. Conversely, the internal capsule and pyramidal tract of the brainstem and cerebellar white mater were relatively spared. Immunostaining for GFAP (Dako, Glostrup, Denmark) showed no or only slight proliferation of reactive astrocytes in the cerebral cortex and white matter lesion (Fig. 2g). Proliferation of reactive astrocytes was slight compared with the severity of tissue degeneration. These pathological findings were observed at almost the same intensity throughout the frontal, temporal and occipital lobes. No fat-laden macrophages or metachromatic substance were evident. No arteriolosclerosis or infiltration of inflammatory cells was evident in the cerebral white matter. Senile plaques and neurofibrillary tangles were not observed in the hippocampus. These pathological findings were consistent with hepatic encephalopathy and final diagnosis was PSE without portal hypertension and liver cirrhosis.